SECED 2023 Conference
Earthquake Engineering & Dynamics for a Sustainable Future
14-15 September 2023, Cambridge, UK

NONLINEAR SEISMIC ANALYSIS OF A SPENT FUEL POOL CONSIDERING STRUCTURE-FLUID-STRUCTURE INTERACTION

Tsvetan Genov[1], Joao Travanca[2], Stoyan Andreev[3] & Anton Andonov[4]

Abstract: *The objective of the paper is to assess approaches to include the effect of fluid-structure along with equipment-fluid-structure interaction by evaluating the response of a typical spent fuel pool found in PWR type reactor auxiliary building to earthquake loading, as well as to derive the seismic demand in critical structural members for the needs of a seismic fragility analysis. Different approaches are presented to account for fluid-structure interaction during the dynamic nature of seismic loading. All structural key aspects considered relevant are included in the analyses: the concrete box structure, the outlining stainless-steel liner, its connections, the submerged rack's structure, and the containing fluid. Three numerical models were developed and tested with the finite element code LS-Dyna with different implementations considering the fluid-structure interaction to demonstrate the robustness of the structure against earthquakes. Mechanical analogue adopted in codes with spring-mass system representation of the fluid attached to the structure and explicit modelling of the domain representing the water considering the two-way interaction between structure and fluid. It is of great importance to include all the effects of fluid-structure interaction, as they increase the response and load of the structure. Both approaches considered for fluid representation were found to capture accurately the global response of the structure. The lattice structure of the racks exerts extra damping in the fluid motion and the pressure loading on the tank walls in near vicinity during earthquake excitation. The explicit modelling approach for the fluid elements could possibly results in lowering the racks critical displacements.*

INTORDUCTION

Spent fuel storage is of a great importance in the different stages of nuclear fuel cycle. At-reactor wet storage pools are widely implemented and fully integrated in the reactor operation, which supervene the seismic qualification. The storage pool is a reinforced concrete structure usually lined with stainless steel that has as primary safety function to provide leak-tightness. The pool is filled with deionized water in which spent fuel bundles vertically arranged in storage racks are kept after its removal from the reactor core for cooling. Storage racks retain the fuel elements together and provide seismic restraint.

The excitation of the spent fuel pool structure causes two-way interaction with the fluid contained. The dynamic behaviour of the liquid can be simplified by a combination of two modes: the impulsive and the convective one. The methods adopted in ACI 350.3-06 (2006), ASCE 4-16 (2016) make use of lumped masses for both impulsive and convective modes and springs for the latter, both capturing the global response of the structure. These approaches were the first practical ones for assessing the hydrodynamic pressures for both cylindrical and rectangular tanks proposed by Housner (1963). The investigations of fluid-structure interaction phenomena were started by Westergaard (1938) with deriving the pressure acting on dam walls during earthquake excitation. Calculation of the effective hydrodynamic masses for the fluid inside a cylindrical tank and cylindrical piers surrounded by fluid was done by Jacobsen (1949). Later Haroun (1983), conducted experimental research on several tanks under dynamic excitation, proposing precise analytical solution for the impulsive pressure. Before the work of Veletsos (1977) the referred analysis of FSI would normally assume rigid walls. Such assumption results in unconservative assessment of the hydrodynamic forces and consequently undedaterestimation of stress demand in the lined structure Epstein (1976).

As the racks are submerged and in contact with fluid, they are expected to exhibit different dynamic properties than in air like medium. The dynamic effects on the submerged structures are of great complexity with various applicable functional dependency on geometrical, stiffness,

[1] Structural Engineer, Mott MacDonald, Bulgaria (Tsvetan.Genov@mottmac.com)

arrangement, boundary condition, flow velocity, relative motion between members. During acceleration, racks tend to exert combination of motions as rocking, overturning, sliding and extra inertial effects are induced by the fluid structure interaction. Generally, a simplification is presented in terms of added mass and damping from the submersion, which assumes the hydrodynamic forces on the bodies Dong (1978).

As an alternative, with the current numerical techniques explicitly simulated fluid can be implemented to assess the response of the structure. Both fluid-structure and equipment-fluid-structure interaction can be investigated. LS-Dyna, a general-purpose 3D finite element software LSTC (2009) was used to develop and analyse both types of representation for the FSI problem.

NUMERICAL MODELS

SFP concrete geometry

The model shown in Figure 1 is an accurate representation of a typical spent fuel pool. Some adjacent structural members are included to model boundary conditions and stiffening effects for SFP floor slab and walls more accurately. For simplicity only the water containing structure is analysed here. The structure consists of concrete walls and slabs with thickness values representative of those usually expected for nuclear auxiliary buildings. Therefore, the parts are modelled with eight node (hexahedral) solid elements. The mesh size of the structural elements was defined based on frequency response analysis, following the recommendation of Section C3.1.3.2 of ASCE (2016), so that a correct mesh size allows for extraction of stresses and forces in all structural members.

Liner and anchoring details

The liner steel plates are meshed with solid elements, elastic material with specific steel properties is assigned. Sliding contacts are defined between the liner plates and the concrete walls and floor with coefficient of friction equal to 0.45.

The embedded angles providing constraint of the liner are modelled with elastic material and thickness 10mm. Only the flanges parallel to the concrete surface are considered, and these are constrained in the solid elements representing the concrete. The gates between the SFP and the surrounding areas are also represented in a simplified manner, as steel plates, with no special details modelled.

The model of the liner with gates is shown in Figure 4.

Spent fuel storage racks

The spent fuel racks are modelled with solid elements, resembling its true shape. High density racks are presented with total usable capacity of around 1070 cells. The corresponding mass of the fuel bundles were considered by increasing the density of the rack material. The explicit rack modelling allows the interaction between the racks and the floor of the pool to be captured with the possibility of assessing the potential tearing, punching of the floor lining, on top of the inertia effects. The racks are modelled as rigid since their response under fluid loading is expected to be elastic, with negligible effects on the FSI calculation and reduction of computation costs. Furthermore, with the fluid being explicitly modelled and with the racks placed close to the wall, pressure anomalies can be assessed in the trapped fluid between the structural wall and racks possibly leading to extra pressure exerted on the tank. The rack model is shown in Figure 3.

The interaction between the fuel racks and the SFP floor liner is modelled with sliding contact, with a friction coefficient of 0.2 based on published research data from reports.

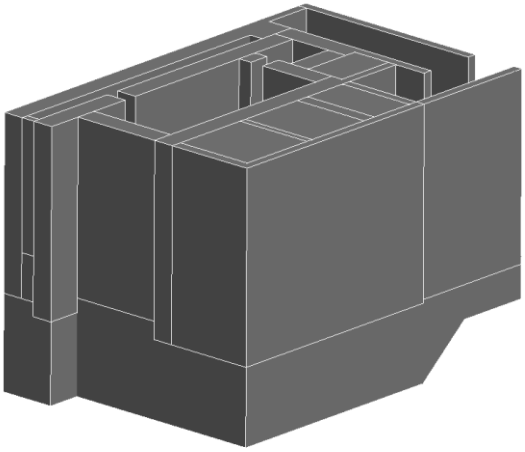

Figure 1 SFP concrete geometry

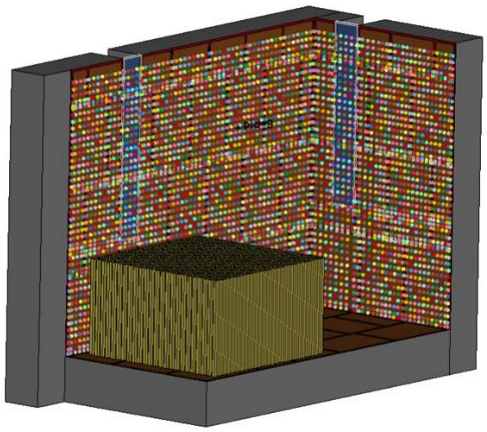

Figure 2 Spent fuel pool side view

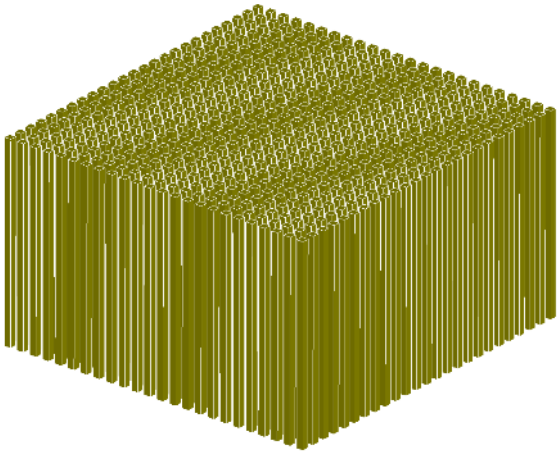

Figure 3 Spent fuel pool storage racks

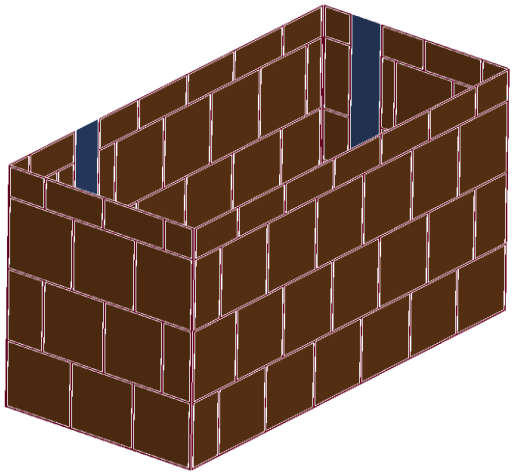

Figure 4 Spent fuel pool stainless steel liner

FSI representation

The approach adopted by codes for the fluid structure interaction problem treats the fluid as added mass, consequently changing the characteristic mass of the structure. The masses accelerated during dynamic loading exert hydrodynamic pressures on the walls, which can be separated into impulsive and convective components. The impulsive pressure is associated with inertial movement of the tank walls, thus the masses assumed are rigidly connected to the tank walls. The convective pressures are associated with the oscillations of the fluid, thus the masses assumed are connected via springs do the walls, with stiffness properly assigned to produce the period of vibration corresponding to the fluid sloshing mode.

Owing to the interest in local stress effects, both impulsive and convective pressures along the wall height are calculated and the respective masses are distributed to account for these pressures, resulting in approximately 9100 springs along the tank walls for the convective part. The vertical fluid modes are assumed to be out of the significant frequency response range and thus for vertical motion the water mass is lumped at the floor slab. The section of the liner finite element model with distributed springs is shown on Figure 5.

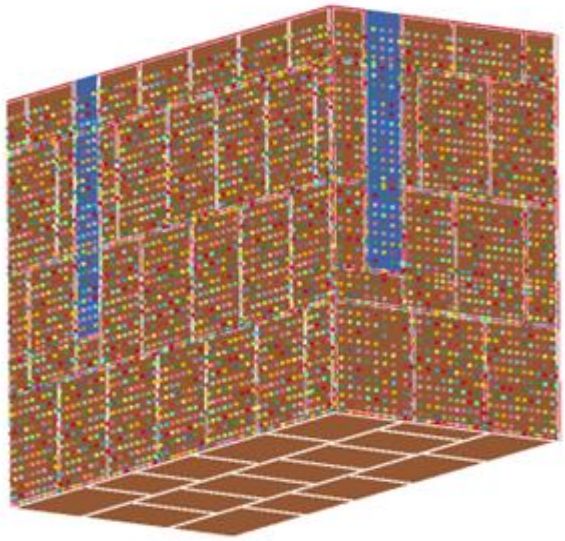

Figure 5 Spring mass finite element model section

In addition to the mechanical representation of the fluid structure interaction, a finite element model was developed with explicit modelling of the fluid elements to address limitations arising in the spring-mass approach, such as the racks to wall and the trapped fluid between interaction which could exert additional pressures on the tank walls from the rack movement. The Incompressible Fluid Dynamic Solver (ICFD) of Ls-Dyna was chosen mainly because of its implicit nature since the ALE approach for mesh movement and the magnitude of the work required from analyst to build and tune the highly non-linear problem. Other available options were considered such as ALE and SPH formulations. The ALE approach was found to had compatibility issues between fluid-structure interface and the other contact types, also high noise oscillation reported in different papers. The latter was found for the SPH approach along with the need of very fine mesh resulting in high computational cost. As the problem focused on interaction, proper no-slip boundary conditions were applied on the interfaces and the corresponding fluid structure interaction cards used to engage coupling between the structural and fluid solvers. Mass and viscosity properties were assigned to the water material, the air was assumed to have zero properties,

. The two sub-domains used in the analyses can be seen on Figure 6 and Figure 7, with the rack included and without the rack.

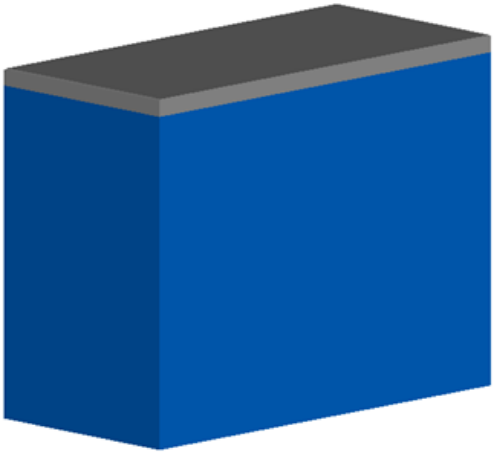

Figure 6 FEM of the explicit fluid domain without racks modelled

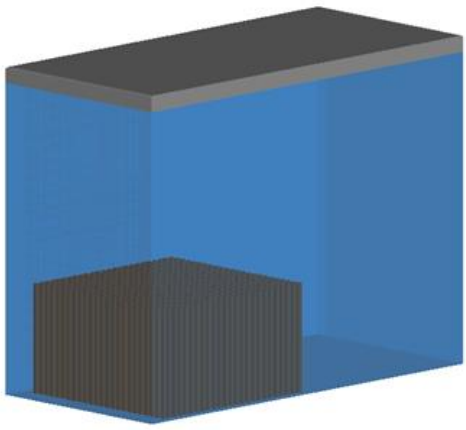

Figure 7 FEM of the explicit fluid domain with racks included

	Volume [m3]	**Density[kg/m3]**	**Viscosity**
Water	1534.48	998.28	0.00105
Air	75	0	0
Total	1609.48	-	-

Table 1 Fluid domain properties

Loading

The loading for all the finite element models is derived in a two-step process: the gravity load is firstly initialized through a linear ramp function, followed by constant 1 second gravity function to damp any excessive oscillations in the model; In the second step the acceleration time histories were applied. Three component acceleration time-histories were used matching the probabilistic ISRS as per NUREG-0800, only one set with truncated duration is presented here for brevity.

NUMERICAL ANALYSES AND RESULTS

Modal analysis

The proposed distribution of the spring-mass system was verified against the code adopted one-directional assembly with one rigidly fastened mass, and one mass connected through springs with stiffness calculated accordingly. Results from the two FEMs first two convective modes of the spring-mass systems and analytical calculated values are listed in Table 2, showing similar values for the first natural frequency in the three cases.

Approach	**1st convective mode [Hz]**	**2nd convective mode [Hz]**
Analytical	0.215	0.315
Code spring-mass system	0.215	0.315
Distributed spring-mass system	0.219	0.310

Table 2 Eigenvalue results

Acceleration response of the concrete structure

The similarity in the seismic response was selected as primary since the liner stresses of interest are induced by static and transient deformation of the concrete structure. The response between the models was assessed in terms of acceleration in-structure response spectra and time histories on the top elevation of the concrete structure to verify the dynamic similarity of the two models.

The response of the models is closely following the phase of the input motion. The results for the two models are identical for frequencies less than 8-10 Hz and start to deviate in the high frequency range 10-30Hz. The higher spectral response of the spring-mass system approach is expected due to the impulsive fluid mass being lumped in the structural nodes.

The explicit modelling of the fluid, lacking the excessive oscillation from lumped masses and the periodic out of phase motion of the fluid and the structure leads to reduction of the higher frequency response of the SFP structural walls. This can be seen in Figure 8, Figure 9, Figure 10(dashed line representing the demand ISRS on top):

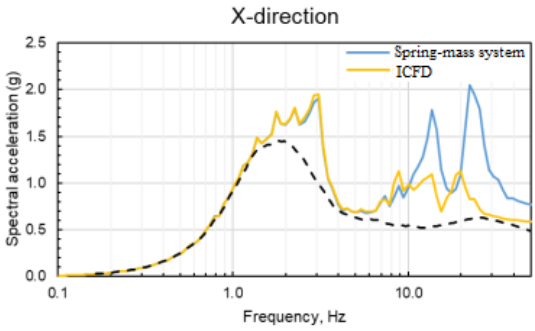

Figure 8 In-structure spectra at top elevation concrete supporting structure – X direction

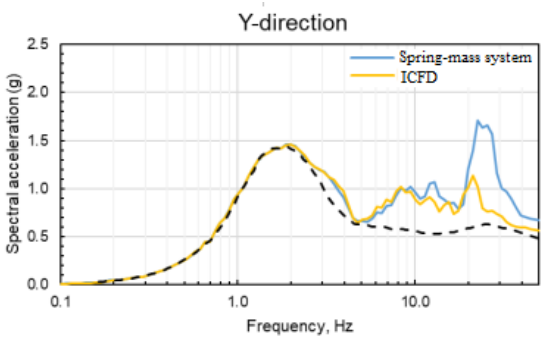

Figure 9 In-structure spectra at top elevation concrete supporting structure – Y direction

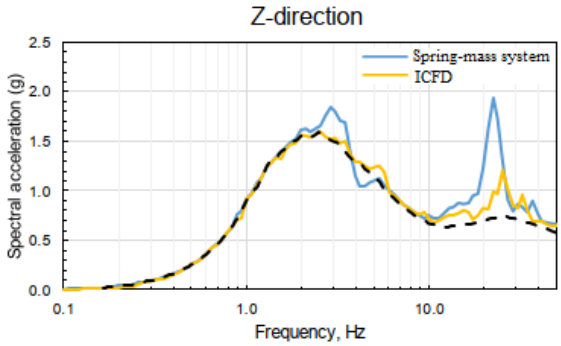

Figure 10 In-structure spectra at top elevation concrete supporting structure – Z direction

Acceleration response of the liner system

The movement of selected points on the liner plates covering the tank walls acceleration time history is presented, the response is following closely the phase of the input motion, resulting in almost identical oscillation between the ICFD and spring-mass system models.

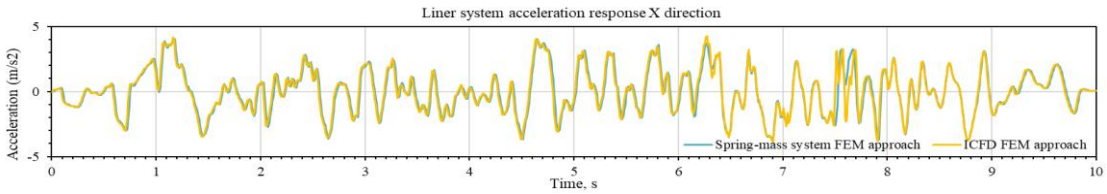

Figure 11 Comparison of the two FEM`s liner structure acceleration time histories – X direction

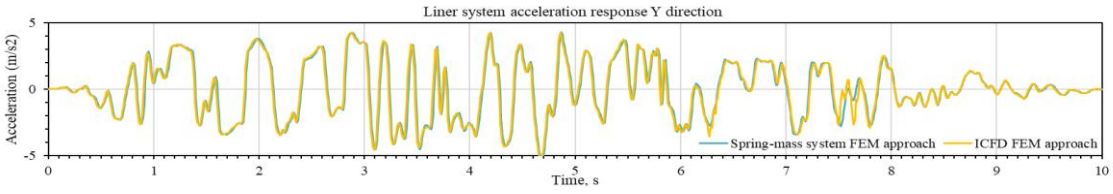

Figure 12 Comparison of the two FEM`s liner structure acceleration time histories – Y direction

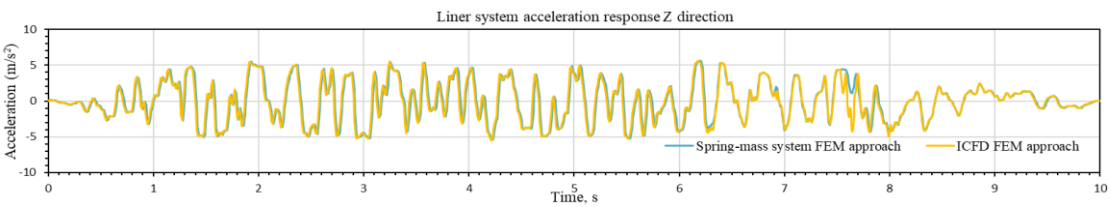

Figure 13 Comparison of the two FEM`s liner structure acceleration time histories – Z direction

Acceleration response of the racks

The sliding response of the racks is essentially the same in both models, some increase of damping is observed in the explicit modelling approach of the fluid, as the racks are deeply submerged are expected to oscillate inertially with the impulsive portion of the fluid domain. Due to the lattice structure of the racks no major drag forces were depicted from the analysis results.

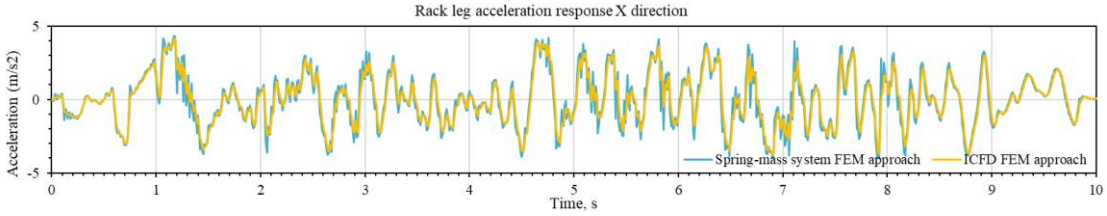

Figure 14 Comparison of the two FEM`s rack leg acceleration time histories – X direction

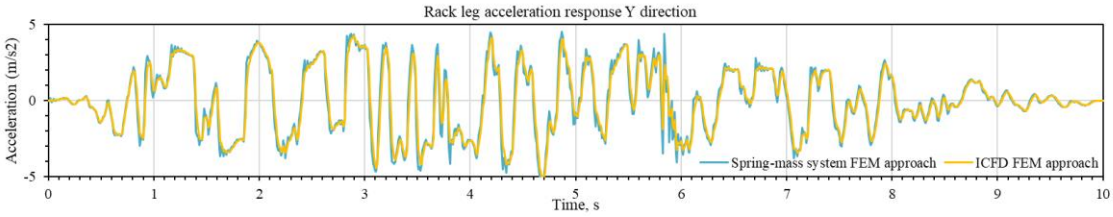

Figure 15 Comparison of the two FEM`s rack leg acceleration time histories – Y direction

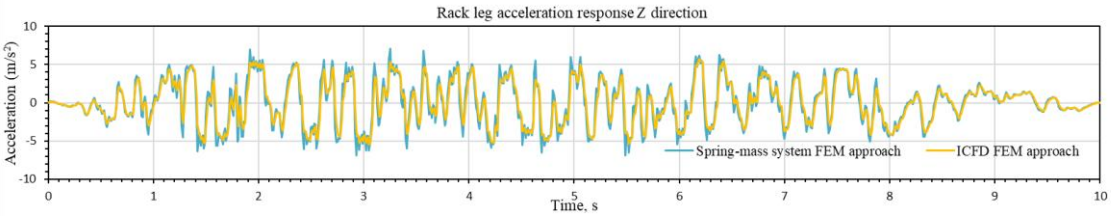

Figure 16 Comparison of the two FEM`s rack leg acceleration time histories- Z direction

Stress response of the liner

Although the acceleration response of the liner was found identical between the spring-mass system and the ICFD approach, the corresponding deformed shape during the static loading part of the analysis differentiate between the models. Also, the drawbacks relating to the rigid wall assumption are observed along with the one-way interaction in the spring-mass system. It is possible that the non-linear interface defined in the ICFD approach amplify the stresses in the liner. Due to the significant difference between the two approaches further analyses are required to confirm the results from the FEM analyses.

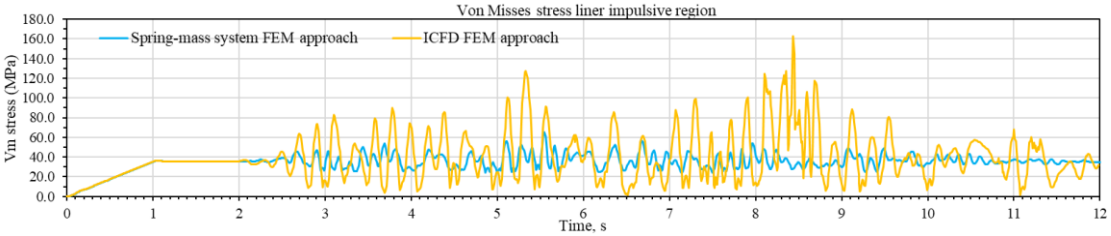

Figure 17 Comparison of VM stresses on the liner in the impulsive region

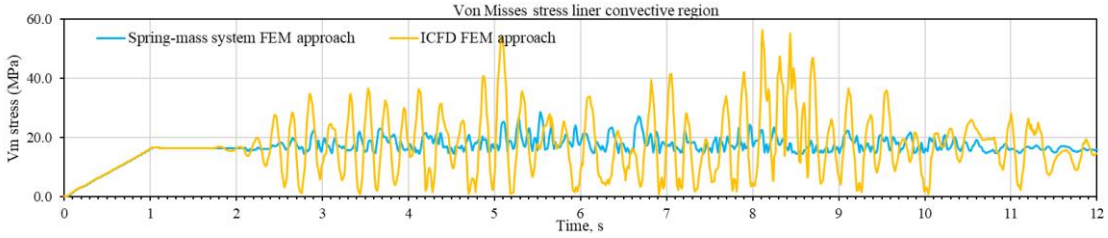

Figure 18 Comparison of VM stresses on the liner in the convective region

Pressure exerted on the tank walls

The hydrostatic and peak hydrodynamic pressures on the SFP walls and floor were compared from the two FEM`s with ICFD formulation of the fluid shown on Figure 19. Analytical calculation of the fluid pressures during the static phase shows good agreement with the numerical results. The variation between the two ICFD models is studied at depth of approximately 9 m below the surface at the tank walls against the racks. This should give an indication of the close to wall positioning and effects from the rack movement. From the results, it can be observed that the models give similar pressure profiles, although the racks tend to act as barrier and some reducing of the pressure exerted on the tank walls from the fluid is depicted. Also, the pressures on the wall far from the racks were assessed, resulting in identical values between the two models

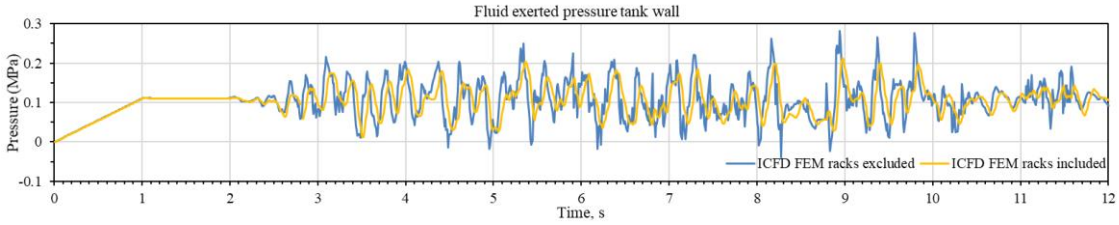

Figure 19 Fluid pressures comparison exerted on the tank walls between the two ICFD FEMs

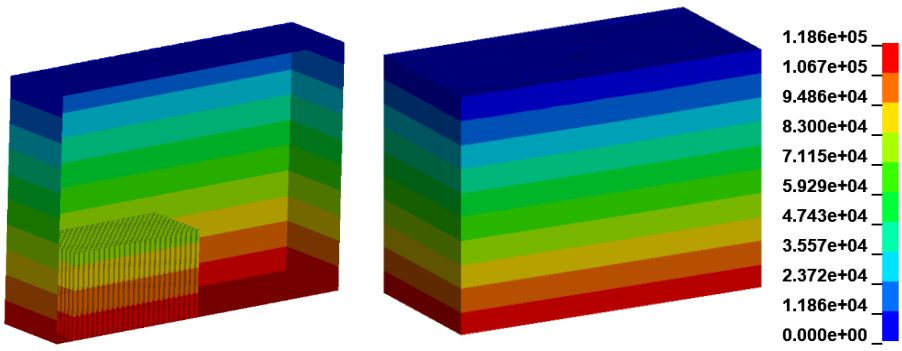

Figure 20 Static fluid pressure racks included *Figure 21 Static fluid pressure racks excluded*

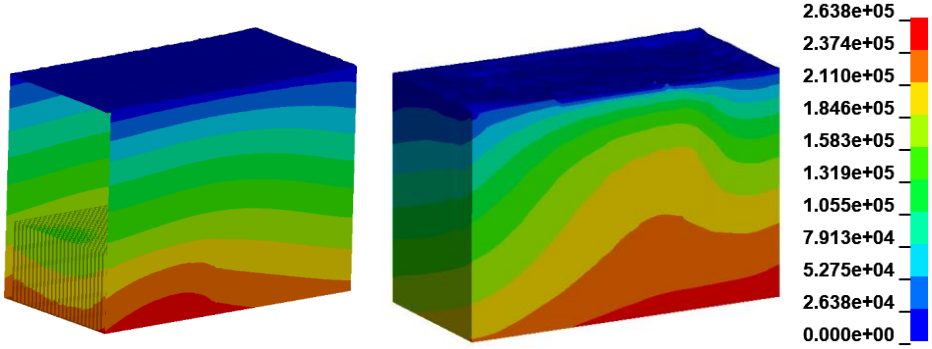

Figure 22 Dynamic fluid pressure racks included *Figure 23 Dynamic fluid pressure racks excluded*

CONCLUSION

The main concept of this research study is to present a coupled approach for tackling all the key aspects of the earthquake response of a typical SFP. The global response of the models is identical in the lower frequency range and only deviate in the high frequency range, due to the oscillations of the lumped masses in the spring-mass approach. The periodic out-of-phase motion of the fluid in the ICFD approach leads to reduction in the high frequency response. It is concluded that both methods are adequate for the needs of the dynamic analysis and represent the global response accurately enough, although the simplified methods seem to be more biased to the conservative side if the SFP structural members failure modes are studied. Disadvantage of the spring-mass approach is the one-way interaction, hence the acceleration of the fluid caused by the structure is not reflected in the fluid pressure. Hence the case with lining the inside of the SFP will results in lower stress evaluations. The fluid interaction with the rack structure could decrease their critical movement. As the mass and inertia of the fluid mainly influence the structure, simplified methods representing the fluid will often be sufficiently reproducing accurate results. However, since these results are only based on the numerical simulations it is necessary to demonstrate the validity and robustness of the assembly by future research.

References

ACI 350.3-06 (2006). Seismic design of liquid-containing concrete structures (ACI 350.3-06) and commentary. American Concrete Institute (ACI) Committee 350, Environmental Engineering Concrete Structures, Farmington Hills, Mich.

ASCE (2016). Seismic Analysis of Safety-Related Nuclear Structures and Commentary, ASCE Standard 4-16, American Society of Civil Engineers.

Housner, G.W. (1963). The dynamic behaviour of water tanks, Bulletin of the Seismological Society of America, 52:3, 381-387.

Westergaard, H.M. (1938). Water pressure on dams during earthquakes, American society of civil engineers. 98,418-433.

Jacobsen, L.S. (1949). Impulsive hydrodynamics of fluid inside a cylindrical tank and of a fluid surrounding a cylindrical pier, Bull. Seism. Soc. Am., Vol. 39.

Haroun, M.A. (1983). Vibration studies and tests of liquid storage tanks. Earthquake Engineering and Structural Dynamics, 11, 190-206.

Veletsos, A.S. Yang, J.Y. (1977). Earthquake response of liquid storage tanks, advances in civil engineering through mechanics, ASCE Proceedings of the second engineering mechanics specially conference, Raleigh, NCL 1-24.

Veletsos, A.S. Tang, Y. and Tang, H.T. (1992). Dynamic response of flexible supported liquid storage tanks. ASCE Journal of Structural Engineering, 118: 264-28.

Epstein, H.I. (1976). Seismic design of liquid-storage tanks, Journal of the Structural Division, 102(9): 1659-167.

Dong, R.G. (1978). Effective mass and damping of submerged structures

Livermore Software Technology Corporation (LSTC) (2019), LS-DYNA Theory Manual

U.S.N.R.C., Standard Review Plan for the Review of Safety Analysis Reports for Nuclear Power Plants: LWR Edition – Design of Structures, Components, Equipment, and Systems (NUREG-0800, Chapter 3), United States Nuclear Regulatory Commission.